

FACILE FUNCTIONALIZATION OF COTTON FABRICS WITH HIERARCHICAL FLOWER-LIKE $\text{Ag}_2\text{Ti}_3\text{O}_7$ LAYER FOR ENHANCED PHOTOCATALYTIC ACTIVITIES UNDER VISIBLE LIGHT IRRADIATION

MOUHEB SBOUI, MOHAMED FAOUZI NSIB,^{*,**} and TSUYOSHI OCHIAI^{***,****}

University of Sfax, Faculty of Sciences, BP1171-3018 Sfax, Tunisia

**National School of Engineers (ENIG), University of Gabès, 6029 Gabès, Tunisia*

***High School of Sciences and Technology of Hammam Sousse, University of Sousse, Tunisia*

****Kawasaki Technical Support Department, Local Independent Administrative Agency, Kanagawa Institute of Industrial Science and Technology (KISTEC), Ground Floor East Wing, Innovation Center Building, KSP, 3-2-1 Sakado, Takatsu-ku, Kawasaki City, Kanagawa 213-0012, Japan*

*****Photocatalysis International Research Center, Tokyo University of Science, 2641 Yamazaki, Noda, Chiba 278-8510, Japan*

✉ *Corresponding author: M. Sboui, sboui.mouheb@gmail.com*

Received October 2, 2019

This paper reports on a facile method for the immobilization of flower-like $\text{Ag}_2\text{Ti}_3\text{O}_7$ architectures on cotton fabric by a mild alkali hydrothermal process at 130 °C, followed by ion exchange in an aqueous solution at room temperature. Evidence of the generation of silver titanate ($\text{Ag}_2\text{Ti}_3\text{O}_7$) was obtained by Raman and XPS, and the morphology of the appended structure was analyzed by FE-SEM. The photocatalytic activity of the titanate material under sunlight stimulant was evaluated with the photodegradation of four models of organic molecules, including Rhodamine B (RhB), phenol (Ph), aniline (AN) and benzoic acid (BA). The Ag^+ doped sodium titanate exhibited remarkable photocatalytic activity in the degradation of organic molecules under both sunlight and visible light irradiations.

Keywords: $\text{Ag}_2\text{Ti}_3\text{O}_7$, photocatalytic activity, cotton, ion exchange, surface functionalization

INTRODUCTION

Alkaline titanates have received a lot of attention due to their potential applications and their unique physical and chemical properties.¹ Sodium trititanate ($\text{Na}_2\text{Ti}_3\text{O}_7$), for instance, finds use in sodium-ion batteries,²⁻⁴ supercapacitors,⁵ chemical absorbents,⁶ photocatalysts and humidity sensors.⁷⁻⁹

For photocatalysis, the powder type of sodium titanate nanostructures with higher surface-to-volume ratio can enhance high performance photocatalytic activity, but some issues in the practical applications need to be overcome, such as separation, aggregation, and recycling.^{8,9} In addition, handicapped by its high band gap ($E_g = 3.70$ eV), $\text{Na}_2\text{Ti}_3\text{O}_7$ lacks activity in the visible light,¹⁰ limiting its photocatalytic activity mainly to UV light.

The immobilization of $\text{Na}_2\text{Ti}_3\text{O}_7$ on an inert support is a good way to recover the catalyst and overcome the problem of powder filtration. It also provides flexibility in photocatalyst handling and

in its use for water purification systems. Among the substrates, cotton fibers have received great attention owing to their low price, abundance, flexibility and lightness.¹¹ All these attributes make the cotton fiber substrate very attractive when compared to traditional rigid substrates. So far, the immobilization of $\text{Na}_2\text{Ti}_3\text{O}_7$ on cotton fibers has never been reported in the literature, probably because of the high temperature or long duration conditions used for the synthesis of $\text{Na}_2\text{Ti}_3\text{O}_7$ based catalyst.

To make the $\text{Na}_2\text{Ti}_3\text{O}_7$ able to effectively use natural sunlight, the ion exchange process can be considered as an alternative to shift the catalyst activation to the visible domain.

Ion exchange is a well-known technique used in many fields, such as the removal of toxic substances and the collection of valuable elements from water.¹²⁻¹⁴ However, this technique can be used for slowing the rate of electron-hole recombination and extending the absorption of

light to the visible range.¹⁰ In particular, titanate materials are commonly used as ion exchangers^{15–22} for these purposes.

For these reasons, it is interesting to investigate how the ion exchange process, involving Ag^+ ion with sodium titanate ($\text{Na}_2\text{Ti}_3\text{O}_7$) immobilized on cotton fabric, is likely to affect the photocatalytic properties of the hybrid Cotton– $\text{Na}_2\text{Ti}_3\text{O}_7$, especially that no data have been reported in this regard. So, to our knowledge, this is the first work reporting on the synthesis, characterization and application of hybrid Cotton– $\text{Ag}_2\text{Ti}_3\text{O}_7$ as photocatalyst. In general, the aim of this research has been to study how the ion exchange process would affect the efficiency of photoactive $\text{Na}_2\text{Ti}_3\text{O}_7$ -containing cotton for the treatment of contaminated water.

In the present work, hybrid systems composed of flower-like $\text{Ag}_2\text{Ti}_3\text{O}_7$ architectures on cotton were prepared and analyzed using different techniques: FE-SEM, Raman, XPS and GSDR. Finally, the photocatalytic activity of the Cotton– $\text{Ag}_2\text{Ti}_3\text{O}_7$ hybrid systems was evaluated for the degradation of four model organic molecules, including Rhodamine B (RhB), phenol (Ph), aniline (AN) and benzoic acid (BA), in water under Xenon lamp irradiation (sunlight simulator).

EXPERIMENTAL

Materials

All chemical reagents (furnished by Aldrich) were of analytical grade and were used without further purification: tetrabutyl titanate (97%), silver nitrate ($\geq 99.8\%$), acetic acid ($\geq 99.7\%$), tert-butanol ($\geq 99.0\%$), NaOH, Rhodamine B (RhB), phenol (Ph), aniline (AN) and benzoic acid (BA). Cotton fabrics were current gauze bandages with sizes of 10 cm \times 10 cm and cellulose content exceeding 99%.

Catalyst preparation

Preparation of Cotton– TiO_2

In order to remove the absorbed water, the cotton samples were dried at 70 °C for 4 h and then immediately dipped into a 1.25 (w/v)% solution of $\text{Ti}(\text{O}i\text{Bu})_4$ in a mixture tert-butanol and acetic acid (90/10 wt%) for 12 h. The samples were then removed and dried at 60 °C for 2 h in an oven and then transferred into a Teflon lined autoclave at 120 °C for hydrothermal treatment during 3 h. After drying in the oven at 50 °C for 2 h, the final material was labeled as Cotton– TiO_2 .

Preparation of Cotton– $\text{Ag}_2\text{Ti}_3\text{O}_7$ flower-like structure

The preparation route for Cotton– $\text{Na}_2\text{Ti}_3\text{O}_7$ is as follows: Cotton– TiO_2 samples were immersed in 80

mL of 10 M NaOH aqueous solution and autoclaved at 130 °C for 4 h in a Teflon lined autoclave. After cooling to room temperature, the material was washed thoroughly with distilled water. After drying in the oven at 60 °C for 3 h, the final material, labeled as Cotton– $\text{Na}_2\text{Ti}_3\text{O}_7$, was recovered and used for photocatalytic tests.

The Cotton– $\text{Ag}_2\text{Ti}_3\text{O}_7$ flower-like structure was prepared by substitution of Na^+ in the sodium titanate films with Ag^+ at room temperature. Typically, Cotton– $\text{Na}_2\text{Ti}_3\text{O}_7$ samples were immersed in 80 mL of 0.1 M AgNO_3 solution at room temperature for 12 h. After the ion exchange process, the materials were washed thoroughly with distilled water to remove excessive ions adsorbed on the surface. After drying in the oven at 60 °C for 3 h, the final material, labeled as Cotton– $\text{Ag}_2\text{Ti}_3\text{O}_7$, was recovered and used for photocatalytic tests.

Characterization

A morphological study of the sample was carried out using a field emission scanning electron microscope (FE-SEM). Images were obtained with a ZEISS SUPRA40, which is completely controlled from a computer workstation. The electron source, a hot cathode producing electrons by the Schottky effect, is a tungsten filament coated with a ZrO layer. Images were processed using SMARTSEM software.

Raman spectra were recorded on a LabRAM Analytical Raman micro-spectrograph (Jobin-Yvon, Horiba group, France), using a He-Ne laser source as exciting radiation ($\lambda = 632.8$ nm) and an air cooled CCD detector. The acquisition time was 100 s.

The X-ray photoelectron spectroscopy (XPS) analysis of the prepared samples was performed using a VG Microtech ESCA 3000Multilab, equipped with a dual Mg/Al anode. The spectra were generated by the unmonochromatized Al K α source (1486.7 eV) run at 14 kV and 15 mA. The analyser operated in the constant energy (CAE) mode. For the individual peak energy regions, a pass energy of 20 eV set across the hemispheres was used. Survey spectra were measured at 50 eV pass energy.

The optical properties of the prepared sample were evaluated using a Perkin Elmer Lambda 35 spectrophotometer operating system between 200 and 700 nm. The reflectance R was obtained from each sample in the UV-vis spectral regions and the remission function F(R) was calculated using the Kubelka–Munk equation for optically thick samples.

Photocatalysis studies

The photocatalytic studies were performed according to the following procedure. A piece of cotton fabric (6 cm \times 6 cm) was immersed in a crystallizer containing 50 mL of 5×10^{-5} M aqueous solutions of four different organic compounds

(Rhodamine B (RhB), phenol (Ph), aniline (AN) and benzoic acid (BA)). Before irradiation, the catalyst was kept in the solution in the dark for one hour to reach adsorption–desorption equilibrium. The system was then illuminated by a 50 W Xenon lamp placed at 10 cm from the top of the beaker. During the photodegradation process, samples were collected from the solution at constant time intervals. A UV–Vis spectrometer (Lambda 35 Perkin–Elmer Spectrophotometer) was used to measure the organic compounds concentration before and after degradation.

RESULTS AND DISCUSSION

SEM observations

The FE–SEM images of the cotton fibers prior and after functionalization with $\text{Ag}_2\text{Ti}_3\text{O}_7$ are shown in Figure 1. Uniform cellulose fibers with smooth surface of the untreated cotton are shown in Figure 1 A. A higher magnification of the cotton fibers is shown in Figure 1 B, where

bundles of the cellulose microfibrils are structured in different cell wall layers.

After functionalization with $\text{Ag}_2\text{Ti}_3\text{O}_7$, the details of the cellulose fibers were no longer visible, revealing the existence of a continuous layer of titanates with microflower structure covering the cellulosic surface (Fig. 1 C). Higher magnification (Fig. 1 D) revealed many flower-like structures composed of many sparsely and randomly arranged thin nanopetals.

Raman spectroscopy

The Raman spectra of neat cotton, Cotton– TiO_2 , Cotton– $\text{Na}_2\text{Ti}_3\text{O}_7$ and Cotton– $\text{Ag}_2\text{Ti}_3\text{O}_7$ are shown in Figure 2. The neat cotton spectrum shows the typical bands of cellulose I at 329, 352, 379, 437, 1295, 1477, 1094 and 1116 cm^{-1} , which is in agreement with literature data.^{23–25}

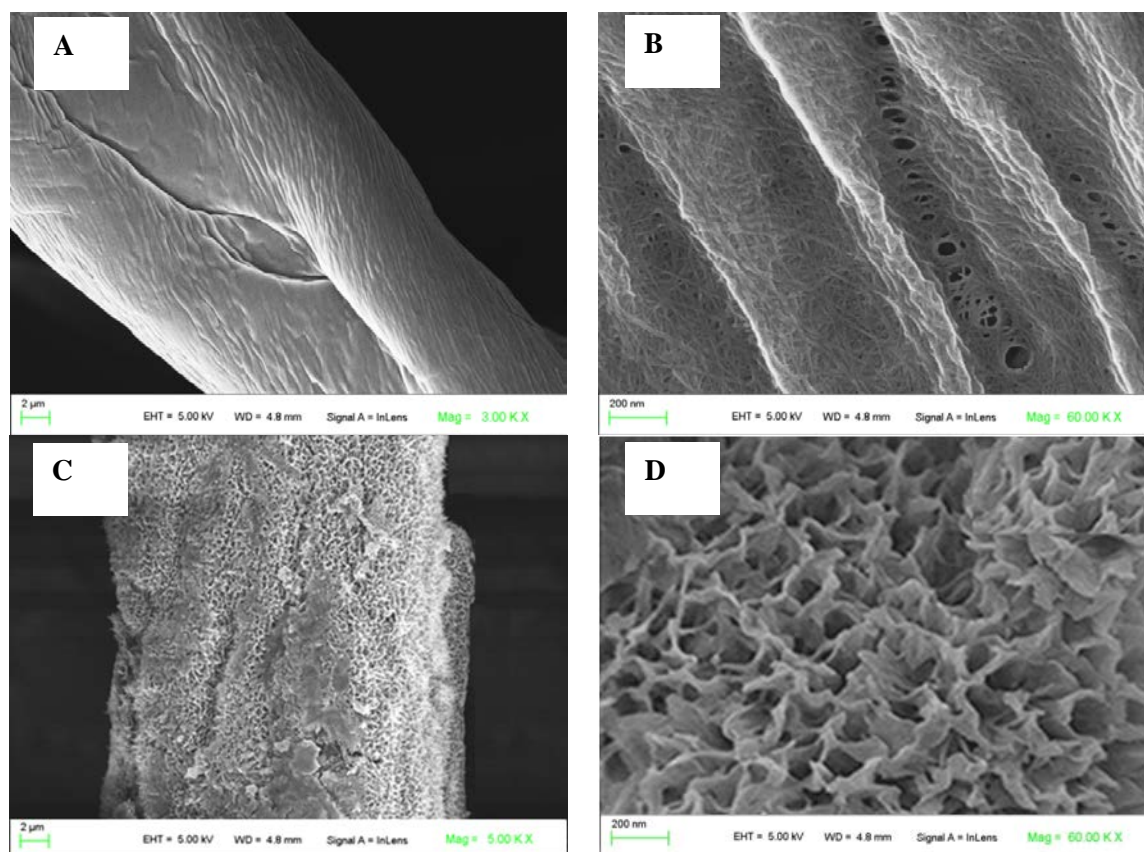


Figure 1: FE-SEM images of neat cotton (A, B) and Cotton– $\text{Ag}_2\text{Ti}_3\text{O}_7$ (C, D)

In the Cotton– TiO_2 spectrum (Fig. 2b), new bands appeared beside those of cellulose I. These new bands at 147, 516 and 637 cm^{-1} correspond to TiO_2 anatase phase.^{25–27} After the mild alkaline hydrothermal treatment, cellulose I was converted

to cellulose II (Fig. 2c) with a shift in the methylene group band from 1477 cm^{-1} in cellulose I to 1461 cm^{-1} in cellulose II.^{24,28} The band relative to the twisting mode of methylene groups at 1295 cm^{-1} in cellulose I was also shifted

to 1265 cm^{-1} in cellulose II. Furthermore, a change of the Raman signal was observed at 379 and 437 cm^{-1} .²⁴

On the other hand, six broad bands appeared in the spectrum of the Cotton- $\text{Na}_2\text{Ti}_3\text{O}_7$ sample (Fig. 2c). These vibration bands are located at 195 , 280 , 442 , 650 , 703 and 900 cm^{-1} and are in good agreement with the data regarding $\text{Na}_2\text{Ti}_3\text{O}_7$ reported in the literature.^{29,30} The band at 195

cm^{-1} is attributed to the Na-O-Ti bending modes,³¹ and the band at 442 cm^{-1} corresponds to the framework Ti-O-Ti vibrations.^{6,32} The bands at 280 , 650 and 703 cm^{-1} are assigned to Ti-O-Ti stretching in edge-shared TiO_6 octahedra.^{6,31-37} The band at about 900 cm^{-1} is assigned to the stretching vibration of terminal short Ti-O bonds involving non-bridging O atoms that are coordinated with Na^+ ions.^{38,39}

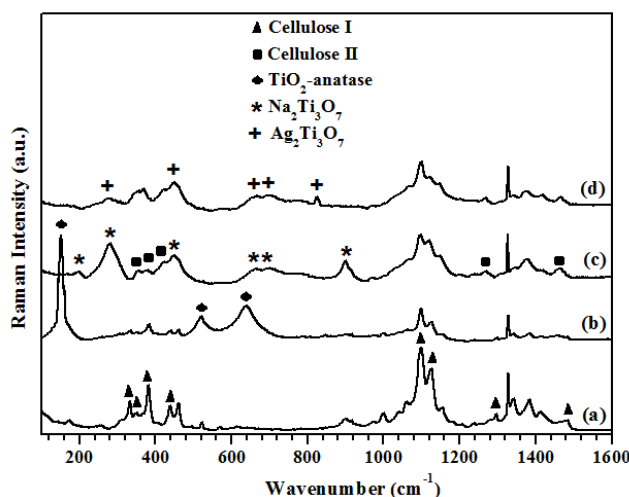


Figure 2: Raman spectra of neat cotton (a), Cotton- TiO_2 (b), Cotton- $\text{Na}_2\text{Ti}_3\text{O}_7$ (c) and Cotton- $\text{Ag}_2\text{Ti}_3\text{O}_7$ (d)

Consequently, Raman analysis further confirmed that $\text{Na}_2\text{Ti}_3\text{O}_7$ grew on cotton fiber after the alkali hydrothermal treatment of Cotton- TiO_2 at $130\text{ }^\circ\text{C}$, indicating that all the TiO_2 phase was turned to $\text{Na}_2\text{Ti}_3\text{O}_7$. After silver ion substitution (Fig. 2d), two bands (195 and 900 cm^{-1}) disappeared, while the other vibration bands remained at the same position, but with a decrease in their relative intensities, in addition to a new band that appears at 824 cm^{-1} . This observation, in agreement with literature data,^{37,38} indicated that the initial titanate layer nanostructure is still retained, except that sodium ions have been discharged and substituted with silver ones.

X-ray photoelectron spectroscopy analysis

The surface chemical compositions of Cotton- $\text{Na}_2\text{Ti}_3\text{O}_7$ and Cotton- $\text{Ag}_2\text{Ti}_3\text{O}_7$ were analyzed by XPS (Fig. 3). The XPS regions analyzed in detail were the Na 1s and Ag 3d bands. As shown in Figure 3, $\text{Na}_2\text{Ti}_3\text{O}_7$ is composed of C, Ti, O and Na, where the presence of carbon (C) mainly comes from cotton.

After silver ion substitution, the sodium peak (1071.4 eV) disappeared, while new peaks related to the Ag element appeared, indicating that the sodium ions have been discharged from the

titanate layers and replaced by silver ions. The other vibration bands remained in the same position.

In the high-resolution XPS spectrum of Ag 3d, the two peaks at 368 and 374 eV usually assigned to Ag $3d_{5/2}$ and Ag $3d_{3/2}$ of the Ag^+ ions^{37,40} were noted, while no peaks corresponding to Ag⁰ species were observed. These findings confirm that the silver species existed as Ag cations on the surface of the Cotton- $\text{Ag}_2\text{Ti}_3\text{O}_7$. All these results, in agreement with the Raman findings, show again the success of the ion substitution process of sodium ions with silver ones, and give evidence of complete conversion of $\text{Na}_2\text{Ti}_3\text{O}_7$ to $\text{Ag}_2\text{Ti}_3\text{O}_7$.

UV-vis characterization

The optical properties of Cotton- $\text{Na}_2\text{Ti}_3\text{O}_7$ and Cotton- $\text{Ag}_2\text{Ti}_3\text{O}_7$ hybrid systems were assessed by ground state diffuse reflectance absorption spectroscopy (GSDR), as shown in Figure 4. Cotton- $\text{Na}_2\text{Ti}_3\text{O}_7$ showed a strong absorption in the UV domain from 250 to 350 nm due to the transition from the O^{2-} anti-bonding orbital to the lowest empty orbital of Ti^{4+} .⁴¹ In Cotton- $\text{Ag}_2\text{Ti}_3\text{O}_7$, a strong and large absorption extending from 400 to 500 nm could be observed, in

addition to the absorption in the UV domain, which is due to the ion exchange process between Na and Ag ions. The valence band of sodium titanate is formed by O 2p orbitals, while the conduction band is formed by Ti 3d orbitals.⁴²

When Na ions are exchanged with Ag ions, the 5s orbitals of Ag are mixed with O 2p orbitals, resulting in an up-shift of the valence band edge and then in a decrease of the band gap energy.⁴³

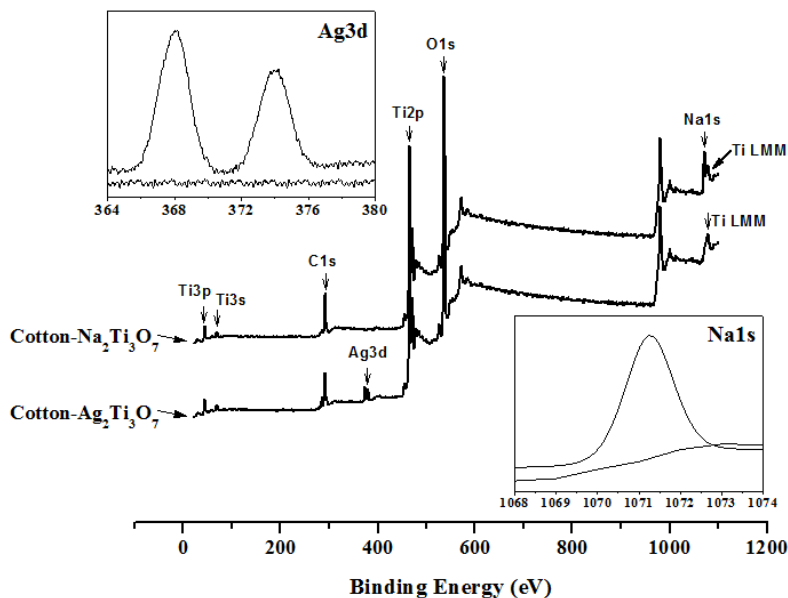


Figure 3: XPS survey of Cotton- $\text{Na}_2\text{Ti}_3\text{O}_7$ and Cotton- $\text{Ag}_2\text{Ti}_3\text{O}_7$; insets present the magnification of Na 1s and Ag 3d regions

The extended absorbance of Cotton- $\text{Ag}_2\text{Ti}_3\text{O}_7$ to the visible range is expected to have a beneficial effect on the photocatalytic activity of the $\text{Ag}_2\text{Ti}_3\text{O}_7$ composite under visible light.

Photocatalytic activity

For the evaluation of the photocatalytic activity of Cotton- $\text{Na}_2\text{Ti}_3\text{O}_7$ and Cotton- $\text{Ag}_2\text{Ti}_3\text{O}_7$, the Rhodamine B (RhB) solution has been selected as a representative organic pollutant to study its photodegradation under a Xenon lamp.

Prior to irradiation, the RhB solution with the composite cotton catalysts was kept in the dark for 1 h to achieve an equilibrium adsorption state. It is worth noting that the adsorbed amount of RhB did not exceed 6% for Cotton- $\text{Na}_2\text{Ti}_3\text{O}_7$ nor for Cotton- $\text{Ag}_2\text{Ti}_3\text{O}_7$, which is indicative of the low adsorption capacity of the prepared hybrid catalysts.

The photocatalytic activity test in Figure 5 (a) reveals that the RhB solution was totally degraded by Cotton- $\text{Ag}_2\text{Ti}_3\text{O}_7$ after 3 h of illumination, while only about 34% of RhB solution was degraded under the same conditions by the Cotton- $\text{Na}_2\text{Ti}_3\text{O}_7$. The Cotton- $\text{Ag}_2\text{Ti}_3\text{O}_7$ exhibited higher photocatalytic activity in the

decomposition of RhB solution. In addition, the photodegradation of the RhB solution exhibited an exponential decay with irradiation time under sunlight irradiation. The photodegradation rate can be described by a first-order reaction (Eq. 1):

$$\ln(C_0/C) = kt \quad (1)$$

where k is the photodegradation rate constant (min^{-1}), C_0 is the initial concentration of RhB solution, and C is the actual concentration of RhB solution at irradiation time t .

The linear relationships between $\ln(C_0/C)$ and the irradiation time are displayed in Figure 5 (b) and the rate-constant values (k) are calculated (see Table 1). The k value for Cotton- $\text{Ag}_2\text{Ti}_3\text{O}_7$ was about 8 times higher than that of Cotton- $\text{Na}_2\text{Ti}_3\text{O}_7$, confirming the strong beneficial role of the ion exchange process involving Ag^+ with $\text{Na}_2\text{Ti}_3\text{O}_7$ in enhancing the photocatalytic activity under sunlight. In order to confirm the role of the ion exchange process of Na^+ ions with Ag^+ ones in enhancing the photocatalytic activity of the Cotton- $\text{Na}_2\text{Ti}_3\text{O}_7$ composite under visible light, the RhB degradation was investigated and carried out under a Xenon lamp with and without a UV filter. As shown in Figure 6, it was found that when using the UV filter, the photocatalytic

activity was extremely low in the presence of Cotton–Na₂Ti₃O₇ (removal rate lower than 10% after 3 h), while a high level of degradation was maintained when Cotton–Ag₂Ti₃O₇ was used (removal rate exceeding 70% after 3 h). This result clearly confirmed the beneficial effect of the ion exchange process involving Ag⁺ with

Na₂Ti₃O₇ in enhancing the photocatalytic activity under visible light irradiation.

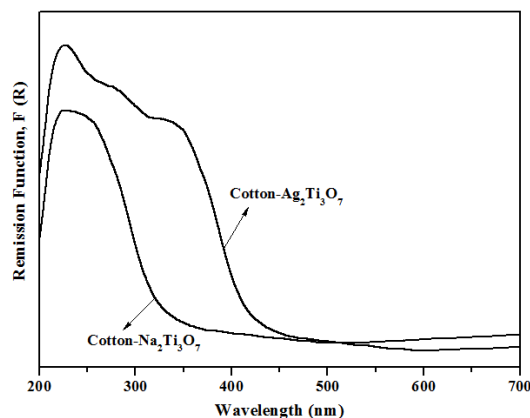


Figure 4: Ground state diffuse reflectance (GSDR) spectra of Cotton–Na₂Ti₃O₇ and Cotton–Ag₂Ti₃O₇

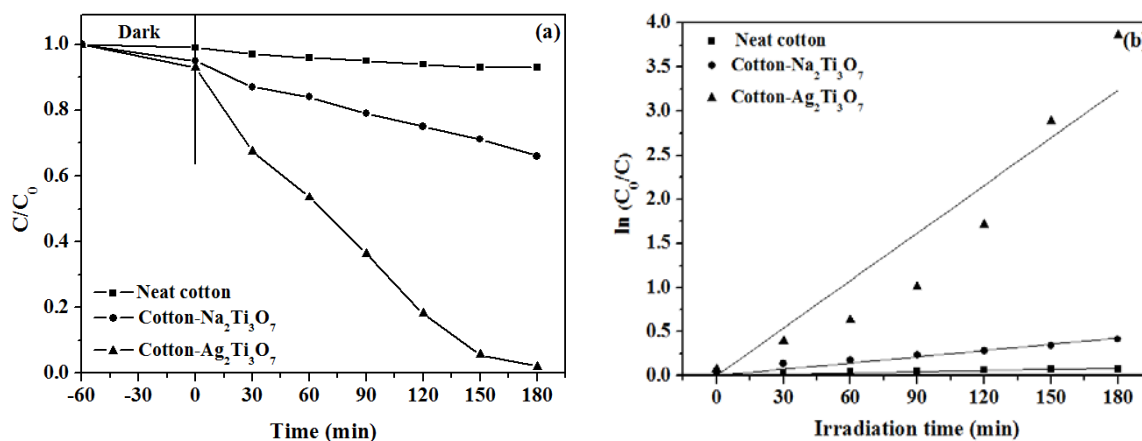


Figure 5: (a) Time dependence of the relative concentration of RhB upon light exposure to sunlight simulator and (b) the kinetic plot of RhB photodegradation in the presence of: neat cotton; Cotton–Na₂Ti₃O₇ and Cotton–Ag₂Ti₃O₇

Table 1
k and R² calculated for RhB photodegradation in the presence of different catalysts

Samples	Kinetic constant (k. min ⁻¹)	R ²
Without catalyst	4.80499x 10 ⁻⁴	0.97
Cotton–Na ₂ Ti ₃ O ₇	0.00239	0.99
Cotton–Ag ₂ Ti ₃ O ₇	0.01799	0.95

The higher activity observed for Cotton–Ag₂Ti₃O₇ is likely due to (i) newly formed intra-band gap states close to the conduction band edge to induce electronic coupling, which prevents the charge recombination, and (ii) to the lower band gap energy of Ag-titanate, compared to Na-titanate after ion exchange with Ag ions,

generating electron-hole pairs after absorption of visible light. As a result, visible light illumination of the Cotton–Ag₂Ti₃O₇ composite generates electrons, which move to the conduction band (CB), while holes move to the valence band (VB). Subsequently, the accumulated electrons in the CB could react with oxygen adsorbed on the

surface to form superoxide anion radicals $\cdot\text{O}_2^-$. Meanwhile, the holes in VB can react with adsorbed H_2O or OH^- species to produce highly reactive $\cdot\text{OH}$ radicals in aqueous solution. These

reactive oxidizing groups can degrade organic pollutants and mineralize it to CO_2 and H_2O , as shown in Figure 7.

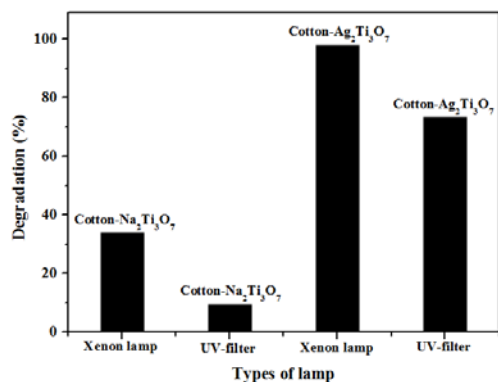


Figure 6: Evolution of RhB concentration in the presence of Cotton- $\text{Na}_2\text{Ti}_3\text{O}_7$ and Cotton- $\text{Ag}_2\text{Ti}_3\text{O}_7$ under Xenon lamp irradiation with and without UV filter

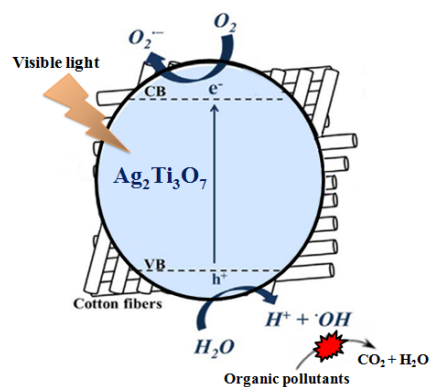


Figure 7: Possible mechanism of the degradation reaction of organic pollutants on Cotton- $\text{Ag}_2\text{Ti}_3\text{O}_7$ photocatalyst

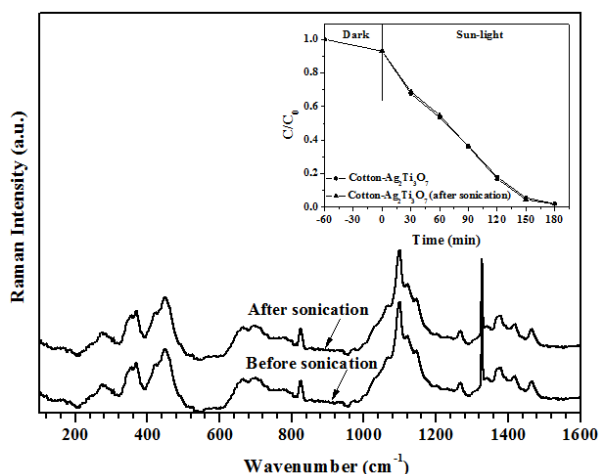


Figure 8: Raman spectra of Cotton- $\text{Ag}_2\text{Ti}_3\text{O}_7$; prior and after sonication for 30 min; inset: evolution of RhB concentration under Xenon light irradiation in the presence of Cotton- $\text{Ag}_2\text{Ti}_3\text{O}_7$; prior and after sonication for 30 min

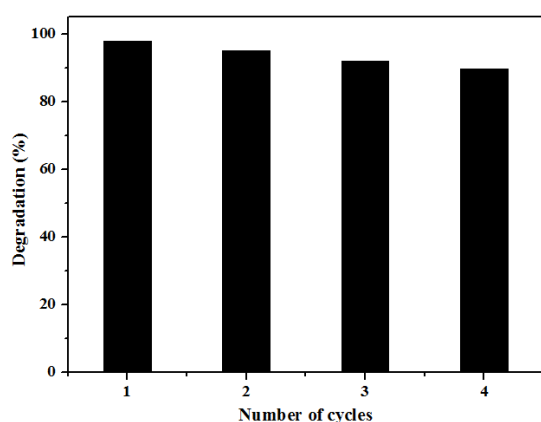


Figure 9: Evolution of photodegradation efficiency of Cotton- $\text{Ag}_2\text{Ti}_3\text{O}_7$ after four cycles of 3 h under Xenon lamp illumination

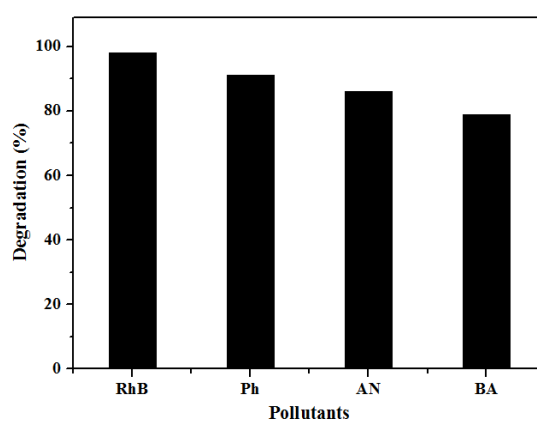


Figure 10: Photodegradation efficiency of some organic pollutants in the presence of Cotton- $\text{Ag}_2\text{Ti}_3\text{O}_7$ irradiated with Xenon lamp illumination

To investigate the stability of the $\text{Ag}_2\text{Ti}_3\text{O}_7$ layer on cotton fibers, an ultrasonic treatment (Power 50 W) was applied to the Cotton– $\text{Ag}_2\text{Ti}_3\text{O}_7$ composite for 30 min. Specifically, the Cotton– $\text{Ag}_2\text{Ti}_3\text{O}_7$ did not show any sign of disintegration nor weakness after the sonication treatment and prolonged contact with water. In particular, the examination of the Raman spectra (Fig. 8) showed the persistence of the $\text{Ag}_2\text{Ti}_3\text{O}_7$ bands with a similar intensity as for the Cotton– $\text{Ag}_2\text{Ti}_3\text{O}_7$ before the sonication treatment. Moreover, there was no change in the photocatalytic efficiency of the Cotton– $\text{Ag}_2\text{Ti}_3\text{O}_7$ sample after the sonication treatment (inset of Fig. 8), confirming the efficient binding of the $\text{Ag}_2\text{Ti}_3\text{O}_7$ layer on the cotton fibers.

Reusability of the photocatalyst

To examine the repeatability of the photocatalytic activity, the Cotton– $\text{Ag}_2\text{Ti}_3\text{O}_7$ composite was used in four consecutive photodegradation cycles of simulated sunlight irradiation during 3 h. After each run, the catalyst was rinsed with water, dried and used again under the same conditions. As shown in Figure 9, the efficiency of the photodegradation process is preserved to an acceptable level after four cycle runs. For instance, the photodegradation rate of RhB attained 89.7% after four cycles, compared to 97.9% for the first run.

Photodegradation tests with other pollutants

The photodegradation of other types of organic pollutants, bearing different functionality, was also investigated in the presence of the Cotton– $\text{Ag}_2\text{Ti}_3\text{O}_7$ photocatalyst, using phenol (Ph), aniline (AN) and benzoic acid (BA). The molecules of these pollutants contain different organic functions, such as phenolic, carboxylic and amine groups.

All the tests were carried out under the same experimental conditions as those with Rhodamine B (RhB). Figure 10 indicates that degradation rates of 98%, 91%, 86% and 79% were attained for Rhodamine B (RhB), phenol (Ph), aniline (AN) and benzoic acid (BA) after 3 h of irradiation, respectively. These results show that the Cotton– $\text{Ag}_2\text{Ti}_3\text{O}_7$ photocatalyst has a very wide applicability for the removal of organic pollutants from wastewater. So, this novel hybrid photocatalyst is very promising and could be employed to remediate contaminated waters using solar irradiation.

CONCLUSION

In this work, an easy and environmentally friendly strategy was introduced to make up flower-like architecture of $\text{Ag}_2\text{Ti}_3\text{O}_7$ arrays, well bound to the cotton fibers. The Cotton– $\text{Ag}_2\text{Ti}_3\text{O}_7$ composite was formed through a mild alkali hydrothermal treatment, followed by the ion exchange process in an aqueous solution at room temperature. The substitution of sodium ions with silver ions has boosted the photocatalytic activity in the visible domain. As a result, Cotton– $\text{Ag}_2\text{Ti}_3\text{O}_7$ exhibited excellent removal capability towards Rhodamine B (RhB), phenol (Ph), aniline (AN) and benzoic acid (BA) in water under simulated sunlight irradiation, suggesting its potential in treating contaminated wastewater. This system is recyclable, flexible, portable, lightweight, economical and biocompatible. Thus, the present study gives rise to a new class of highly efficient hybrid photocatalysts that may practically harvest energy from sunlight.

REFERENCES

- Y. C. Chang, J. C. Lin and S. H. Wu, *J. Alloys Compd.*, **749**, 955 (2018), <https://doi.org/10.1016/j.jallcom.2018.03.332>
- S. Anwer, Y. Huang, J. Liu, J. Liu, M. Xu *et al.*, *ACS Appl. Mater. Interfaces*, **9**, 11669 (2017), <https://doi.org/10.1021/acsami.7b01519>
- P. Senguttuvan, G. Rousse, V. Seznec, J. M. Tarascon and M. R. Palacín, *Chem. Mater.*, **23**, 4109 (2011), <https://doi.org/10.1021/cm202076g>
- A. Rudola, K. Saravanan, C. W. Mason and P. Balaya, *J. Mater. Chem. A*, **1**, 2653 (2013), <https://doi.org/10.1039/C2TA01057G>
- C. Wang, Y. Xi, M. Wang, C. Zhang, X. Wang *et al.*, *Nano Energy*, **28**, 115 (2016), <https://doi.org/10.1016/j.nanoen.2016.08.021>
- M. Feng, W. You, Z. Wu, Q. Chen and H. Zhan, *ACS Appl. Mater. Interfaces*, **5**, 12654 (2013), <https://doi.org/10.1021/am404011k>
- S. Ogura, M. Kohno, K. Sato and Y. Inoue, *J. Mater. Chem.*, **8**, 2335 (1998), <https://doi.org/10.1039/A805172K>
- C. Y. Xu, J. Wu, P. Zhang, S. P. Hu, J. X. Cui *et al.*, *Cryst. Eng. Comm.*, **15**, 3448 (2013), <https://doi.org/10.1039/C3CE27092K>
- V. Štengl, S. Bakardjieva, J. Subrt, E. Vecerníková, L. Szatmary *et al.*, *Appl. Catal. B*, **63**, 20 (2006), <https://doi.org/10.1016/j.apcatb.2005.09.006>
- M. Vithal, S. Rama Krishna, G. Ravi, S. Palla, R. Velchuri *et al.*, *Ceram. Int.*, **39**, 8429 (2013), <https://doi.org/10.1016/j.ceramint.2013.04.025>
- G. Goncalves, P. A. A. P. Marques, R. J. B. Printo, T. Trindadea and C. P. Neto, *Compos. Sci. Technol.*,

- 69, 1051 (2009), <https://doi.org/10.1016/j.compscitech.2009.01.020>
- ¹² S. Komarneni and R. Roy, *Nature*, **299**, 707 (1982), <https://doi.org/10.1038/299707a0>
- ¹³ A. Zagorodni, "Ion Exchange Materials: Properties and Applications", Elsevier, Amsterdam, 2006
- ¹⁴ A. M. Wachinski and J. E. Etzel, "Environmental Ion Exchange: Principles and Design", CRC Press, Cleveland, OH, 1997
- ¹⁵ A. Clearfield and J. Lehto, *J. Solid State Chem.*, **73**, 98 (1988), [https://doi.org/10.1016/0022-4596\(88\)90059-X](https://doi.org/10.1016/0022-4596(88)90059-X)
- ¹⁶ A. J. Celestian, D. G. Medvedev, A. Tripathi, J. B. Parise and A. Clearfield, *Nucl. Instrum. Methods Phys. Res. B*, **238**, 61 (2005), <https://doi.org/10.1016/j.nimb.2005.06.019>
- ¹⁷ M. Nyman and D. T. Hobbs, *Chem. Mater.*, **18**, 6425 (2006), <https://doi.org/10.1021/cm061797h>
- ¹⁸ M. Poojary, R. A. Cahill and A. Clearfield, *Chem. Mater.*, **6**, 2364 (1994), <https://doi.org/10.1021/cm00048a024>
- ¹⁹ A. J. Celestian, D. G. Medvedev, A. Tripathi, J. B. Parise and A. Clearfield, *J. Am. Chem. Soc.*, **130**, 11689 (2008), <https://doi.org/10.1021/ja801134a>
- ²⁰ J. Lehto, R. Harjula and A. M. Girard, *Dalton Trans.*, **1**, 101 (1989), <https://doi.org/10.1039/DT9890000101>
- ²¹ D. J. Yang, Z. F. Zheng, H. Y. Zhu, H. W. Liu and X. P. Gao, *Adv. Mater.*, **20**, 2777 (2008), <https://doi.org/10.1002/adma.200702055>
- ²² D. J. Yang, Z. F. Zheng, H. W. Liu, H. Y. Zhu, X. B. Ke *et al.*, *J. Phys. Chem. C*, **112**, 16275 (2008), <https://doi.org/10.1021/jp803826g>
- ²³ Y. Liu, *Analyst*, **123**, 633 (1998), <https://doi.org/10.1039/A707064K>
- ²⁴ K. Schenzel, H. Almlöf and U. Germgard, *Cellulose*, **16**, 407 (2009), <https://doi.org/10.1007/s10570-009-9286-0>
- ²⁵ M. Sboui, S. Bouattour, L. F. Liotta, V. La Parola, M. Gruttadauria *et al.*, *J. Photochem. Photobiol. A*, **350**, 142 (2018), <https://doi.org/10.1016/j.jphotochem.2017.09.074>
- ²⁶ T. Ohsaka, F. Izumi and Y. Fujiki, *J. Raman Spectrosc.*, **7**, 321 (1978), <https://doi.org/10.1002/jrs.1250070606>
- ²⁷ L. L. Lai, W. Wen and J. M. Wu, *Cryst. Eng. Comm.*, **18**, 5195 (2016), <https://doi.org/10.1039/C6CE00578K>
- ²⁸ K. Schenzel and S. Fischer, *Cellulose*, **8**, 49 (2001), <https://doi.org/10.1023/A:1016616920539>
- ²⁹ Y. M. Wang, G. J. Du, H. Liu, D. Liu, S. B. Qin *et al.*, *Adv. Funct. Mater.*, **18**, 1131 (2008), <https://doi.org/10.1002/adfm.200701120>
- ³⁰ H. M. Kim, F. Miyaji, T. Kokubo and T. Nakamura, *J. Ceram. Soc. Jpn.*, **105**, 111 (1997), <https://doi.org/10.2109/jcersj.105.111>
- ³¹ B. C. Viana, O. P. Ferreirab, A. G. S. Filhoc, A. A. Hidalgo, J. M. Filhoc *et al.*, *Vib. Spectrosc.*, **55**, 183 (2011), <https://doi.org/10.1016/j.vibspec.2010.11.007>
- ³² T. Gao, H. Fjellvåg and P. Norby, *Inorg. Chem.*, **48**, 1423 (2009), <https://doi.org/10.1021/ic801508k>
- ³³ B. C. Viana, O. P. Ferreirab, A. G. S. Filhoc, A. A. Hidalgo, J. M. Filhoc *et al.*, *J. Braz. Chem. Soc.*, **20**, 167 (2009), <https://doi.org/10.1590/S0103-50532009000100025>
- ³⁴ Y. V. Kolen'ko, K. A. Kovnir, A. I. Gavrillov, A. V. Garshev, J. Frantti *et al.*, *J. Phys. Chem. B*, **110**, 4030 (2006), <https://doi.org/10.1021/jp055687u>
- ³⁵ J. Xie, T. H. Ji, X. H. Ou-Yang, Z. Y. Xiao and H. J. Shi, *Solid State Commun.*, **147**, 226 (2008), <https://doi.org/10.1016/j.ssc.2008.05.026>
- ³⁶ M. Kitano, E. Wada, K. Nakajima, S. Hayashi, S. Miyazaki *et al.*, *Chem. Mater.*, **25**, 385 (2013), <https://doi.org/10.1021/cm303324b>
- ³⁷ N. Ren, R. Li, L. Chen, G. Wang, D. Liu *et al.*, *J. Mater. Chem.*, **22**, 19151 (2012), <https://doi.org/10.1039/C2JM32434B>
- ³⁸ N. Li, L. Zhang, Y. Chen, M. Fang, J. Zhang *et al.*, *Adv. Funct. Mater.*, **22**, 835 (2012), <https://doi.org/10.1002/adfm.201102272>
- ³⁹ S. Ivanova, A. Penkova, M. D. Hidalgo, J. A. Navío, F. R. Sarria *et al.*, *Appl. Catal. B*, **163**, 23 (2015), <https://doi.org/10.1016/j.apcatb.2014.07.048>
- ⁴⁰ C. W. Bates, G. K. Wertheim and D. N. E. Buchanan, *Phys. Lett. A*, **72**, 178 (1979), [https://doi.org/10.1016/0375-9601\(79\)90686-8](https://doi.org/10.1016/0375-9601(79)90686-8)
- ⁴¹ Y. B. Mao and S. S. Wong, *J. Am. Chem. Soc.*, **128**, 8217 (2006), doi.org/10.1021/ja0607483
- ⁴² Y. An, Z. Li, H. Xiang, Y. Huang and J. Shen, *Cent. Eur. J. Phys.*, **9**, 1488 (2011), <https://doi.org/10.2478/s11534-011-0072-x>
- ⁴³ M. Machida, X. W. Ma, H. Taniguchi, J. Yabunaka and T. Kijima, *J. Mol. Catal. A: Chem.*, **155**, 131 (2000), [https://doi.org/10.1016/S1381-1169\(99\)00329-5](https://doi.org/10.1016/S1381-1169(99)00329-5)